Numerical modeling of the seismic performance of Romanian timber-framed masonry walls

F. Parisse[*1], E. Poletti[1], A. Dutu[2] and H. Rodrigues[3]

[1] Institute for Sustainability and Innovation in Structural-Engineering (ISISE)
Department of Civil Engineering, University of Minho
Campus de Azurém, 4800-058 Guimarães, Portugal
e-mail: francescoparisse3@gmail.com and elisapoletti@civil.uminho.pt
web page: https://www.uminho.pt/PT

[2] Department of Civil Buildings, Technical University of Civil Engineering of Bucharest
Bd. Lacul Tei 122-124, 020396 Bucharest, Romania
e-mail: andreea.dutu@utcb.ro - web page: https://utcb.ro/

[3] RISCO
Department of Civil Engineering, University of Aveiro
Campus Universitário de Santiago, 3810-193 Aveiro, Portugal, Portugal
e-mail: hrodrigues@ua.pt - web page: http://sweet.ua.pt/hrodrigues/

Abstract. *Traditional architecture with timber-framed masonry (TFM) elements' system was used in many seismic countries due to its performance when subjected to earthquakes. Romanian TFM structures can be considered a representative example since they were constructed by local builders applying basic concepts of earthquake-engineering. The seismic assessment of these buildings and even panels still presents many open issues due to the intrinsic properties and complex interaction between materials and elements. Although global behavior is influenced by many factors at local and element scale, TFM walls play an important role in defining the response under dynamic loading such as earthquakes. The present paper aims to investigate the seismic performance of Romanian TFM walls by using a simplified equivalent frame with linear elastic elements and nonlinear properties lumped at the connections. This model was built in OpenSEES software concentrating the non-linear behavior at the joints with a spring per degree of freedom whose parameters were initially calibrated based on representative experimental tests, and then updated until the local and global responses approached those of the experimental campaign performed at the Technical University of Civil Engineering of Bucharest in terms of initial stiffness, maximum base shear, and total dissipated energy. The simplified modeling strategy requires limited computational efforts and provides information about the role of each connection.*

Keywords: Timber-Framed Masonry, Seismic Assessment, Equivalent Frame Method, Lumped Plasticity, Nonlinear Cyclic Analysis

1 Introduction

The construction system consisting of Timber-Framed structures with Masonry infill (TFM) or other composite materials can be considered a product of centuries' long accumulation of knowledge and experience that is passed down through generations of local people from around the world. To this regard, it is one of the oldest vernacular architecture that should be treated and preserved as cultural heritage. Its conservation may be pursued only by understanding the structural and architectural characteristics to respect authenticity of the construction and ensure compatibility for any potential intervention.

Although the TFM system is widespread all over the world and throughout the history, each area shows different features according to the available materials, techniques and knowledge resulting in several structural configurations of timber frame (dimensions and arrangement of wooden elements) and type of infill [1]. Since the vast majority of these structures were built without following any design code or recommendation, in the present section, TFM construction typologies are classified as semi-engineered and non-engineered, even though their configuration may vary in each group from half-timbered type, masonry reinforced with wooden skeleton, to mixed systems between the ground floor and upper stories. The non-engineered TFM buildings can be found in countries with low seismic hazard (Canada, Sweden, Norway, England, Germany - *fachwerk*, France - *colombages*, Spain - *entramados*) sometimes having the timber frames only for aesthetical reason, but they can also be observed in areas prone to severe earthquakes. In this latter case, the timber skeleton plays an important role for dynamic actions acting as a reinforcement of masonry as well as for static ones depending on the structural configuration [1]–[3]. For this reason and other intrinsic characteristics of materials and construction typology such as tensile-resistant properties of timber light weights, and effective connections between elements, TFM structures showed a good seismic behavior that was constantly improved through damage observation and proven by comparing their response with those of different structural typologies [4]. Figure 1 shows the correlation between seismic hazard and TFM structures with basic earthquake-resistant concepts applied by local builders in the reconstruction processes such as those in Albania, Romania (*paianta*), Greece, Turkey with *Hatil*, *Himis* and *Bagdadi* techniques [4]. In Northern Pakistan, *Cator and Cribbage* system and *Bhatar* method were developed and can be defined as masonry reinforced with horizontal timber elements as well as *Taq* technique in Kashmir where another method consisting of patchwork quilt wall, *Dhajji-dewari*, can also be found [5], [6]. Regarding TFM

structures spread across Central and South America, they are known as *Bahareque* in Colombia, *Vareque* in Ecuador, *Pajareque* in Honduras, *Pared Francesa* in Argentina, *Quincha* in Perù, *Adobillo* in Chile and *Taquezal* in Nicaragua [7]–[9].

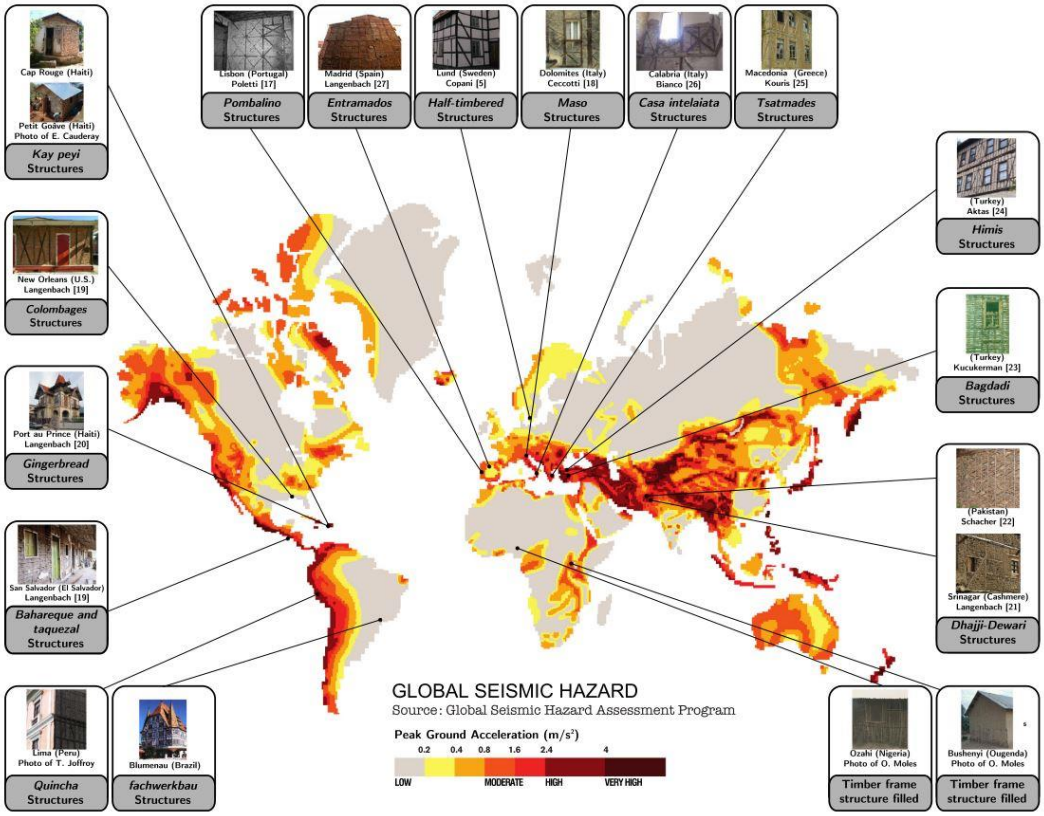

Figure 1 Timber-framed masonry structures [10].

The semi-engineered construction typology was developed in few countries such as Portugal and Italy where the reconstruction process after two severe earthquakes (1755 and 1783 respectively) was led by the corresponding governments that provided guidelines and design recommendations considered the first technical regulations on seismic design [2], [11]. However, the Portuguese *gaiola pombalina* and the Italian *casa Baraccata* differ in terms of configuration because they can be classified as a half-timber structure with masonry infill and a masonry structure reinforced with wooden skeleton, respectively.

Since existing TFM structures showed a good earthquake resistance during past earthquakes [4], their response should be studied both experimentally and numerically to estimate the seismic capacity as well as to predict the potential mechanisms and damages. Although the scientific community has increased its research on this issue, the available experimental tests on TFM walls are limited. Some in-plane quasi-static cyclic tests on *Pombalino* frontal walls were performed by Santos [12], Meireles *et al.* [13], Gonçalves *et al.* [14], Poletti and Vasconcelos [11], Poletti *et al.* [15] studying the influence of infill and vertical loads

applied on the wall showing a hysteretic response with pinching behavior related to strength degradation, high ductility and good dissipation capacity [16]. Moreover, Romanian TFM structures were tested by Dutu *et al.* [17], [18] varying the type of infill and arrangements of timber elements as well as for Turkish TFM walls considering also different timber species and cladding resulting in similar highly ductile responses [19]. Other studies were carried out on Haitian TFM walls by Vieux-Champagne *et al*. [10], *baraccato* system by Ruggeri [20] and *quincha* system by Torrealva and Vicente [21].

The existing numerical models are also limited and can vary in terms of complexity and sensitivity. Kouris and Kappos [22] proposed a detailed nonlinear finite element model validated by experimental tests, but its application requires many input data and experience of users. Simplified approaches were proposed by Kouris and Kappos [22], Ceccotti and Sandhaas [23], Folz and Filiatrault [24], Lukic *et al.* [25] considering linear elastic deformable or rigid elements connected by nonlinear springs calibrated according to cyclic test results on connections and panels.

TFM buildings are still built in Romania and many existing ones have undergone to severe deterioration processes [17], thus they should be studied even more than other structural typologies because there is no recommendation about design and retrofitting strategies that can be followed either by technicians or non-specialized people in the Romanian Building Code. Although Romanian TFM structures have experienced many seismic events, their seismic capacity is still not estimated with numerical studies. This work aims at simulating the in-plane cyclic behavior of Romanian masonry panel by a simplified equivalent frame model with nonlinear springs lumped at the connections. This approach is reliable and applicable to whole buildings, if future studies on the connections will be conducted, since the analyses require few computational efforts.

After a brief building characterization on Romanian TFM architecture, the most representative mixed panel is described as well as its cyclic response resulting from an experimental campaign performed by Dutu *et al.* [26]. The numerical model was calibrated by an inverse fitting procedure based on the measurements and observations collected during the experimental test. This simplified model was built in the software OpenSEES [27] applying the equivalent frame modeling strategy with lumped nonlinearities. These nonlinear properties were calibrated by inverse fitting the numerical cyclic responses with those of representative connections tested by Sakata *et al.* [28], and Dutu *et al.* [29]. After this initial calibration, the

properties were adjusted again to approach the global response of the Romanian TFM wall tested by Dutu *et al.* [17]. The main pros and cons of the simplified modeling strategy and those of inverse fitting procedure are eventually discussed in terms of accuracy and computational effort. Moreover, the applicability of this approach to other TFM structures as well as its possibilities are emphasized by comparing the Romanian mixed system to the Portuguese one in terms of modeling issues and results, namely seismic parameters and damage mechanisms.

2 Romanian Building characterization

The Romanian traditional architecture can be defined as a half-timber masonry structure since its timber skeleton plays an important role under static and dynamic loads [2], [3]. This structural system is known as "*paianta*" consisting of TF panels with bracings and brick masonry infill, which are connected to wooden floor and roof with truss configurations. Starting from "*paianta*" typology, some characteristics have been modified depending on location, availability of materials and construction techniques [17]. Several structural configurations of the timber frame can be observed therefore the dimensions and arrangement of wooden elements, type of infill, and tree species could have varied from structure to structure. These features depend also on the seismic hazard of each area of the country since local builders have improved the seismic performance of TFM constructions by damage observations.

Considering the energy and number of events, Romania can be classified as a country with moderate to high seismic risk with some areas particularly prone to large earthquakes such as Vrancea region in the fore-Arc of Carpathians where the most active tectonic processes are lumped [30]. Vrancea seismic source has produced nine earthquakes with a M_w higher than 7 during the last two centuries with main shock and aftershocks sometimes characterized by comparable magnitude [30]. The focus may range from 90 to150 km according to ROMPLUS seismic catalogue and the maximum expected PGA is 0.4g. TFM buildings located in this area were characterized in their geometrical and structural configuration to understand their earthquake-resistant details and evaluate their seismic capacity.

A field investigation was performed by Dutu *et al.* [17] across the fore-Arc seismic area resulting in five types of TFM houses depending on the their characteristics and infill. In the present paper, the configuration with timber frame with brick masonry infill (Type 1 in [3]) is considered representative of the Romanian TFM architecture (70% of 169 buildings investigated), thus its geometrical and structural features are briefly

described. Figure 2a shows a TFM building classified as Type 1 in Ocnesti with some typical construction details. The mixed panel usually presents bracings not perfectly aligned with the diagonal and just connected to the vertical post, and a mixed perimeter beam at floor or roof level, Figure 2b. It is worth to stress that bracings are effective only in compression since they detach from the frame in tension due to the nailed connections. Masonry infill usually consists of mud bricks burnt in not-industrial ovens whose strength depends on their position inside the oven, and mud based mortar made by mixing raw earth with sand and water, and applied after one day of resting time [17]. The amount or mortar components may vary in each area based on the type of soil. However earth with very significant percentage of clay can be found due to its cohesive and hardness properties when mixing and after curing, respectively. This also means that some minor cracks occur in the setting process and the interaction between brick masonry infill and timber frame is characterized by the lack of adherence, therefore out-of-plane mechanisms are not prevented [17]. Figure 2b shows that infill bond may vary along the height of the panel to increase the friction in the upper part of the wall as well as the stiffness [17]. The superstructure is supported by a stone platform with stringers called "soles" that distribute more uniformly the loads [17]. Moreover, timber joints are mainly half-lap cross-halved or tee-halved type between post and beams, but mortise and tenon type can be also found, Figure 3a and b. Most of the existing buildings were in poor conditions due to moisture related problems leading to irreversible decay of timber elements.

(a) **(b)**

Figure 2 Timber frame geometry of building in Ocnesti (a) and mixed perimeter beam (b) [29].

(a) **(b)**

Figure 3 Tee-halved (a) and mortise and tenon (b) joints [29].

3 Previous experimental campaign on TFM walls

The previous building characterization resulted in the identification of three timber-framed (TF) wall typologies varying the type of infill, whose main geometrical features, materials and constructive techniques were studied to perform an experimental campaign aimed at evaluating their in-plane cyclic behavior.

Four TF panels with different infill, e.g. mud bricks (Specimens S1 in [18] and S2 in [17]), wattle and daub (S2 Specimen in [18]), and earth and straw confined by horizontal strips (S3 Specimen in [18]), as well as arrangement of diagonal elements, namely lower (S1 Specimen in [18]) and corner-to-corner bracings (Specimens S2 in [17] and S3 in [18]), were built by a non-specialized company considering materials, average geometrical dimensions and structural joints comparable with those observed *in situ*. S1 Specimen with mud brick masonry infill and lower diagonals, Figure 4 [18], can be considered representative of Romanian TFM walls since it was found in many buildings during the field investigation in Section 2. So, the correspondent experimental campaign and its results are briefly described and taken as a reference for the following numerical calibration.

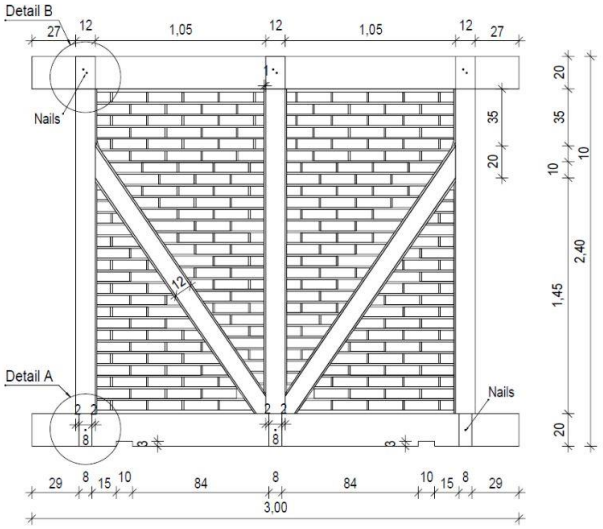

Figure 4 S1 Specimen in [18].

The wall specimen is 3 x 2.4 m in size with slightly smaller dimensions than those observed *in situ* due to the maximum height allowed by the testing frame setup. Timber elements are made of Romanian fir whose mechanical properties were estimated by other experimental campaigns on prisms and beam [29]. Regarding the connections, bottom post-to-beam joints are mortise and tenon type, while the upper ones are half-lap tee-halved type. They are all nailed as well as those linking the diagonal bracings to the columns. Although the construction process was supervised, some imperfections such as gaps were observed at the joints, which may slightly affect the wall global response [18].

The pure shear behavior of Romanian TFM walls was studied by in-plane tests performed in a quasi-static cyclic regime with their setup is described in Dutu *et al.* [17]. An external vertical load of 26 kN was applied by a vertical hydraulic jack and its value can be considered representative of their compressive state. The horizontal displacements were transmitted by two hydraulic jacks following the CUREE Caltech loading protocol [31]. Both vertical loads and horizontal displacements were controlled manually; nevertheless, accurate results were obtained despite the low strength of the wall specimens compared to the reaction frame and a ±20% variation of the vertical load [18].

S1 Specimen showed a ductile response with pinching behavior and no significant damages on timber elements and their connections. Figure 5 pictures the hysteretic curve and its envelope with initial stiffness of 1375 kN/rad, maximum shear capacity of 29 kN and 3.22 kNm in terms of dissipated energy. These properties are influenced by the arrangement of diagonal elements, whose presence modifies the deformed shape, the progression of damages as well as their pattern [18], rather than the type of infill. Local compression perpendicular to the grain was observed in the upper tee-halved joint and pull-out of the diagonal bracing subjected to tension which goes back to the initial position during the reverse cycle. Moreover, a significant vertical sliding of the timber bracings was observed in their upper connection to the external posts influencing the global stiffness, which is not significantly increased by the infill. Indeed it was already cracked almost from the beginning due to shrinkage and it detached from the timber frame after the first cycle since the infill-to-frame adhesion is very low. However, masonry infill can prevent buckling of the diagonals due to its confinement effect and can increase the seismic energy dissipation through shear sliding if the out-of-plane collapse is not activated. The following numerical model was calibrated based on the estimated stiffness, maximum base shear, dissipated energy resulting from the experimental test as well as

local checks were performed to approach the observed damage mechanisms such as diagonal detachment and vertical sliding of bracings.

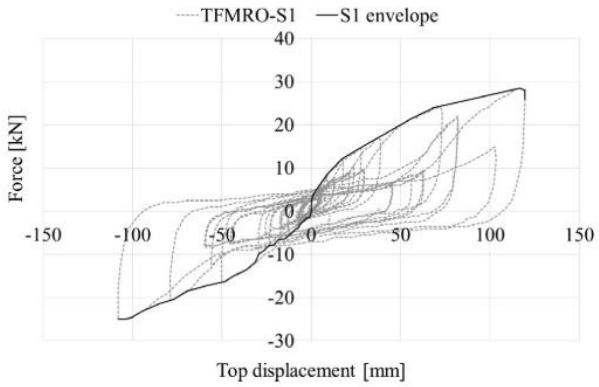

Figure 5 Hysteresis loop and envelope of the first cycle for S1 Specimen [17].

4 Description of numerical model and calibration of its connections

The structural behavior of tested S1 Specimen (masonry infill with lower bracings) by Dutu *et al.* [18] was approached by modeling the panel in OpenSEES [27], an open-source computational platform whose numerical formulation is based on the finite element method, through an equivalent frame with no infill and nonlinear properties lumped at the connections as proposed by Lukic *et al.* [25]. The wall response is mostly influenced by the joint calibration that was performed by the procedure of inverse fitting to achieve a good approximation between the experimental hysteretic curve and the numerical one in terms of initial stiffness, maximum base shear and total dissipated energy.

Since no damage was observed along timber members, they were modeled with linear elastic elements connected by translational and rotational springs with nonlinear hysteretic materials. Masonry infill was not modeled because the deformation capacity of the wall is mainly controlled by the presence and arrangement of timber bracings as reported in Section 3. This assumption provides an underestimation in terms of stiffness due to the masonry confinement effect, and of dissipated energy due to the friction between timber elements and infill and also along the joints.

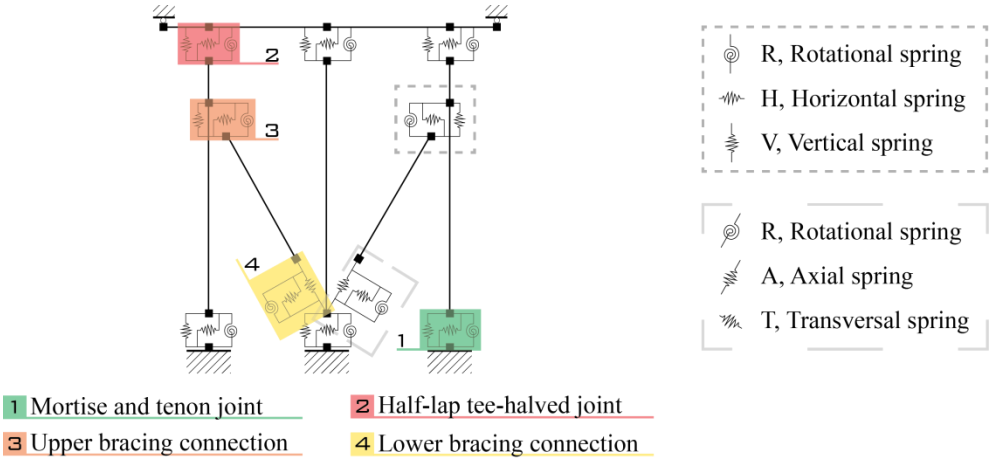

Figure 6 Structural scheme of S1 Specimen.

Figure 6 shows the structural scheme of S1 Specimen with each connection numbered and consisted of three springs, e. g. 1A, 1T, 1R standing for axial, transversal, rotational spring of mortise and tenon type (1), respectively, except for the upper joint between post and bracing (3) where the springs are named as horizontal (H), vertical (V) and rotational (R). The pantograph system of the reaction frame was modeled by two sliding supports at the upper beam ends which prevent any rotation and uplift to simulate the pure shear behavior. The upper beam can be considered as rigid to ensure the same horizontal displacements of timber elements, while bracings are modeled as trusses. They can slide vertically along the external posts until a certain value based on the observation during the test (around 60 mm) and they can detach if subjected to tension since the withdrawal capacity is very low, returning to their initial position in the reverse loading.

The mechanical properties of Romanian fir and those of masonry infill were assumed consistent with experimental tests performed on similar materials [29]. Self weight of masonry was applied at the structural joints considering their tributary area and a specific weight of 19.6 kN/ m^3, while timber elements have specific weight of 385 kg/m^3. Modulus of elasticity parallel to grain direction was assumed equal to 8.9 GPa based on experimental tests on similar timber batches [29].

Since the seismic performance of Romanian TFM walls is strongly affected by the structural joints, the upper connections (2) in Figure 6, and lower ones (1) were calibrated according to the experimental tests on half-lap tee-halved and mortise and tenon type performed by Dutu *et al.* [29] and Sakata *et al.* [28], respectively. Although there are some discrepancies related to geometrical characteristics, types of fasteners and timber species, they can provide a good estimation of the unconfined moment resisting behavior, tensile and shear capacity of both structural joints under in-plane monotonic or cyclic loads. After the initial characterization, the upper (2) and lower (1) connections were adjusted again to approach the local measurements during the

experimental test by Dutu *et al*. [18] such as vertical displacements or rotations of the posts and, at the same time, the global response of the wall. Moreover, the connections between diagonals and timber frame (3), and (4) were calibrated to match the global envelope and, at the same time, the experimental observations such as vertical sliding along the external posts and diagonal detachment from the central lower connection.

4.1 Mortise and tenon joint type (1)

Mortise and tenon joint behavior is highly influenced by the width of the tenon, the dimensions of timber elements, their wood species and the presence of defects or gaps due to the construction process as well as the presence of fasteners such as dowels. Since there are no experimental tests on Romanian mortise and tenon connections, their initial calibration is based on the results of the Japanese experimental campaign by Sakata *et al.* [28] considered as the most representative in terms of geometry and timber species for the moment resisting behavior and tensile capacity. The tests will be briefly presented in this section. Their geometry, setup and loading protocol were reproduced in the software OpenSEES by modeling timber members as linear elastic elements and by applying nonlinear hysteretic materials to the translational and rotational springs simulating the connections.

The Japanese campaign was performed on several configurations of mortise and tenon connection type varying in cross-sectional geometry of beam and post, dimensions of tenon and dowel as well as modulus of elasticity. Their bending behavior was studied by in-plane cyclic tests with one-side actuator transmitting the horizontal load, Figure 7b. The reference M-θ hysteretic curve used for calibration relates to the Specimen named BD-No.5 with dimensions explained in Table 1. This sample has both post and beam made of cedar instead of Romanian fir with comparable moisture content, lower modulus of elasticity parallel to grain and higher bending strength, Table 2. A timber dowel made of hardwood (oak) was applied as fastener to prevent post uplifting, Figure 7a.

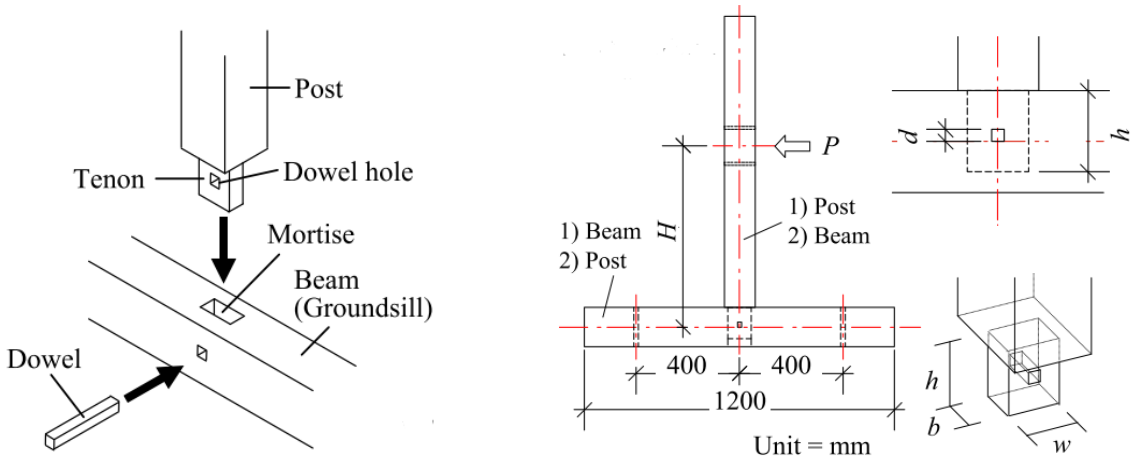

(a) **(b)**

Figure 7 Mortise and tenon connection with timber dowel: elements (a), geometry (b) [28].

252 **Table 1 Dimensions of tested mortise and tenon specimens (in-plane cyclic test) [28].**

Specimen	Post Section [mm]	Beam Section [mm]	Tenon Height h, Width w, Thickness b [mm]	Dowel Section [mm]
BD-No.5	120x120	120x150	120x90x36	18x18
Romanian joint	120x120	200x220	200x80x80	-

253 **Table 2 Material properties of tested mortise and tenon specimens (in-plane cyclic test) [28].**

Tree species	Specific Gravity [-]	Moisture Content [%]	Modulus of elasticity parallel [GPa]	Bending Strength [MPa]
Cedar	0.48	15.7	6.19	39.20
Romanian Fir		15	8.9	-

254 4.1.1 A rotational spring (1R) simulating the moment resistance of mortise and tenon joint

255 The moment resisting behavior of this connection was represented by a rotational spring (1R in Figure 6)
256 whose hysteretic material is *SAWS*, developed by Patxi Uriz, Exponent (Converted from FORTRAN code
257 originally written by Folz and Filiatrault in [32]) while a linear elastic material with large stiffness was
258 defined for the two translational springs. Figure 8a shows the numerical hysteretic curve, highlighted in red,
259 overlapped with the experimental one with a good approximation in terms of initial stiffness and global
260 envelope. The cumulative dissipated energy of both curves was calculated as well as the difference between
261 numerical and experimental cumulative dissipated energy normalized against the experimental one. As can
262 be observed, an underestimation of the numerical model since the first cycles, which results in larger values
263 in the last cycles (-26% for 0.138 rad) due to the different unloading and reloading stiffness, Figure 8b.
264 Eventually, the initial parameters calibrated for *SAWS* material were increased in terms of initial and yielding

stiffness as well as ultimate strength. These adjustments addressed the stiffness underestimation due to the confinement effect of masonry infill.

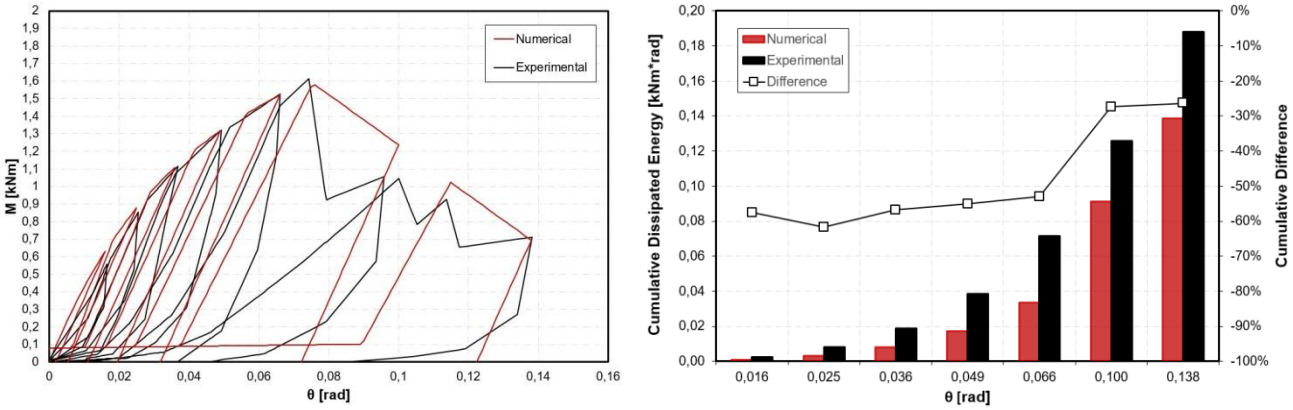

(a) (b)

Figure 8 M- θ hysteretic curves (a) and cumulative dissipated energy (b) for mortise and tenon joint (in-plane cyclic test).

4.1.2 An axial spring (1A) simulating the tensile capacity of mortise and tenon joints

The tensile capacity of mortise and tenon joints was studied by pulling the post out from its initial position following a half-cyclic loading protocol with incremental displacements. In this case, the wooden dowel, previously made of oak, was substituted by a steel one to obtain shear failure mechanism, Figure 9. Table 3Table 3 Dimension of tested mortise and tenon specimens (tensile test). and Table 4 show the geometrical characteristics and material properties of the tested specimens related to the experimental curve named T-No.4 in [28], respectively. This curve is representative of ductile failure among those resulting from the mentioned campaign and was taken as a reference to calibrate the vertical spring of mortise and tenon connection even if it shows a lower strength compared to the experimental curve representative of brittle failure mode.

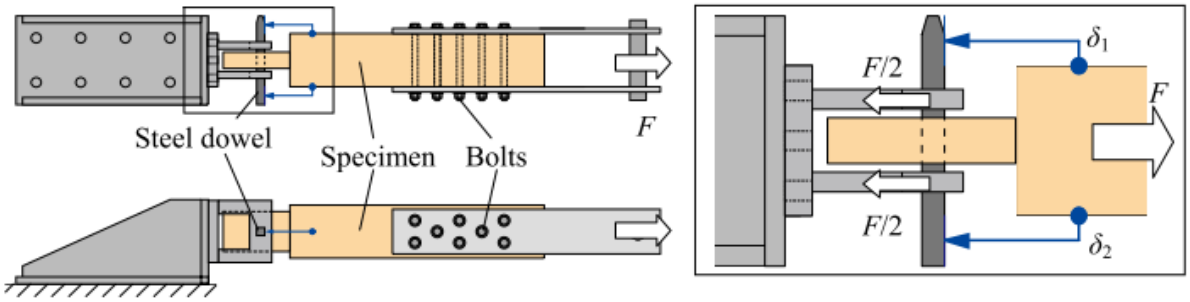

Figure 9 Tension test setup [28].

Table 3 Dimension of tested mortise and tenon specimens (tensile test).

Specimen	Post Section [mm]	Tenon Height h, Width w, Thickness b [mm]	Dowel Section [mm]

T-No.4 in [28]	120x120	150x90x30	18x18
Romanian joint	120x120	200x80x80	-

278 **Table 4 Material properties of tested mortise and tenon specimens (tensile test).**

Tree species	Specific Gravity [-]	Moisture Content [%]	Modulus of elasticity parallel [GPa]	Bending Strength [MPa]
Cedar (CC)	0.41	13.1	6.19	39.20
Romanian Fir		15	8.9	

279 The tensile behavior of this connection was represented by a vertical spring (1A in Figure 6) with hysteretic
280 material *Pinching4* in OpenSEES library, while a linear elastic material with large stiffness was defined for
281 the horizontal and rotational springs. Figure 10a shows the numerical hysteretic curve, in red, perfectly
282 overlapped with the experimental one also resulting comparable in terms of reloading and unloading stiffness
283 even in the last cycles. The cumulative difference decreased to -7.5% for strain values of ε around 0.30%
284 meaning that the two areas are have almost the same value, Figure 10b. The calibrated vertical spring was
285 modified before its application to the wall numerical model since its behavior should be non-symmetric in
286 tension and compression. Thus, the compressive part results from merging the *Pinching4* material in parallel
287 with an *Elastic-No tension* uniaxial material with high compressive stiffness. This means that the
288 compressive response is almost rigid with negligible displacements to prevent the posts going through the
289 bottom beam.

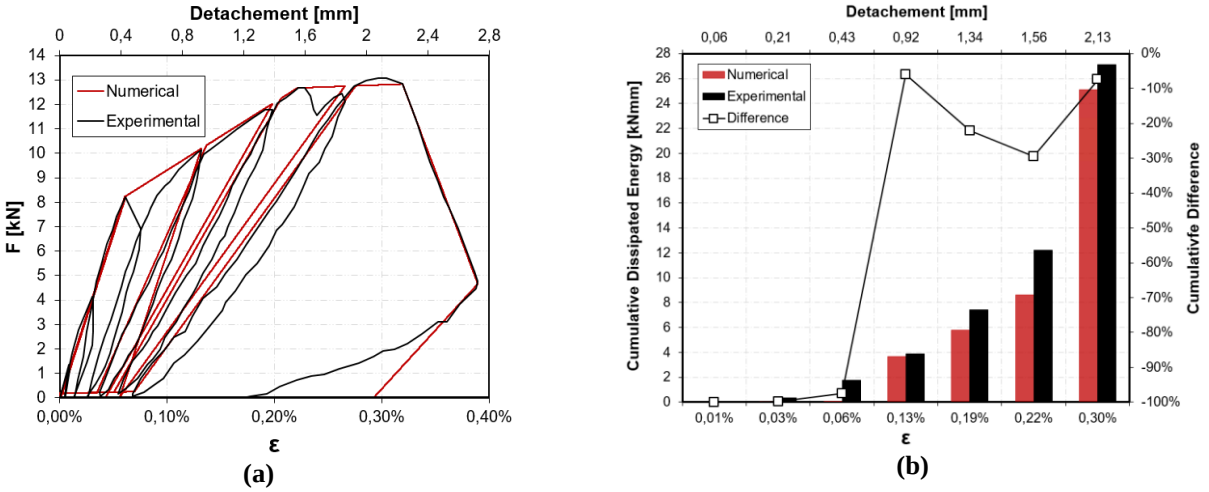

(a) **(b)**

Figure 10 F-δ hysteretic curves for mortise and tenon joint (tensile test).

290 The pull-out strength was also determined as the characteristic load-carrying capacity for nailed timber-to-
291 timber connections with fasteners in double shear according to EN1995-1-1 [33]. The resulted characteristic
292 capacity is around 8.94 kN considering the two plain nails for each connection. Although there are some
293 uncertainties in the estimation of this value such as dimension of nails (assumed as 6 mm), its tensile strength

294 (considered as the minimum value of 600 N/mm^2) and penetration depth (assumed as 40 mm), the ultimate
295 capacity is comparable with the measured pull-out strength of 12.83 kN resulting from the experimental test
296 by Sakata *et al.* [28], thus the connection was not further modified.

297 #### 4.1.3 A transversal spring (1T) in the mortise and tenon joint

298 Regarding the transversal springs of mortise and tenon connection (1T in Figure 6), it was modeled with a
299 linear elastic material with high stiffness (1000 times the modulus of elasticity of timber elements) to prevent
300 any relative displacements between the fixed points and the bottom ends of the posts since there is no
301 relative sliding between post and lower beam.

302 ### 4.2 Half-lap tee-halved type (2)

303 The initial calibration of half-lap tee-halved joints is based on the results of the experimental campaign
304 carried out at Sakata Laboratory of Tokyo Institute of Technology considered as the most representative in
305 terms of geometry and timber species for the moment resisting behavior [29]. The same modeling strategy
306 was applied by means of an equivalent frame model with nonlinear springs at the connections in the software
307 OpenSEES.

308 #### 4.2.1 A rotational spring (2R) simulating the moment resistance of tee-halved joints

309 The bending behavior was studied by in-plane cyclic tests with one actuator transmitting the horizontal load,
310 Figure 11. The specimens were built with timber elements made of fir and cross-sectional dimensions similar
311 to those of Romanian tee-halved joints, Table 5. Since the application of horizontal loading with just an
312 actuator from one side can result in non-symmetric hysteretic curves, the calibration was performed taking as
313 reference the hysteresis with positive forces and displacements.

314 **Table 5 Dimensions of tested tee-halved specimens (in-plane cyclic test).**

Specimen	Post Section [mm]	Beam Section [mm]	Thickness b [mm]
Connections 1-6	120x105	160x105	52.5
Romanian joint	120x120	200x120	60

315

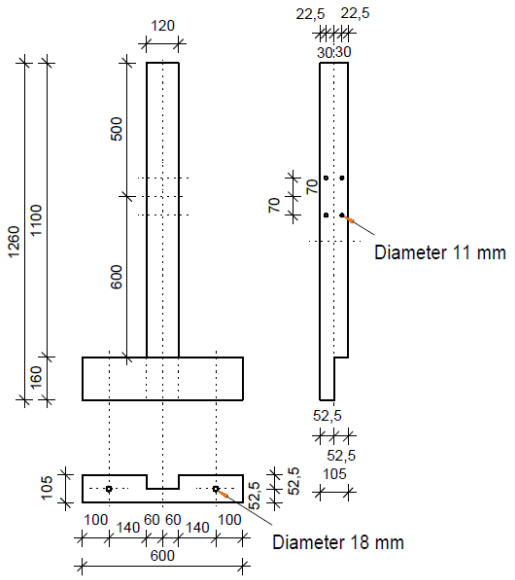

Figure 11 Geometry of tee-halved connection [29].

A rotational spring (2R in Figure 6) represents the moment resisting behavior of tee-halved connection with *SAWS* uniaxial material while both vertical and horizontal ones have a linear elastic material with large stiffness (1000 times the modulus of elasticity of timber elements). Overlapping the experimental and numerical hysteretic curves shows a good approximation in terms of reloading and unloading stiffness even in the last cycles, Figure 12a. The cumulative difference ranges from large values to +13% for drifts (δ) around 30% with the numerical area exceeding the experimental one after around the 7% of δ due to the energy dissipated when the load reverses simulating the pinching effect, Figure 12b. Moreover this difference is a limitation neither of the material model nor of the software, but depends mostly on the initial assumption of considering as reference the cycles with positive forces and displacements whose related cycles are larger than those in the opposite sense. This behavior results from the accumulation of damages in the connection which make its shear capacity and stiffness lower. The parameters of *SAWS* material resulting from the explained calibration were updated in terms of initial and yielding stiffness as well as ultimate strength. These adjustments addressed the stiffness underestimation due to the confinement effect of masonry infill as in Section 4.1.1.

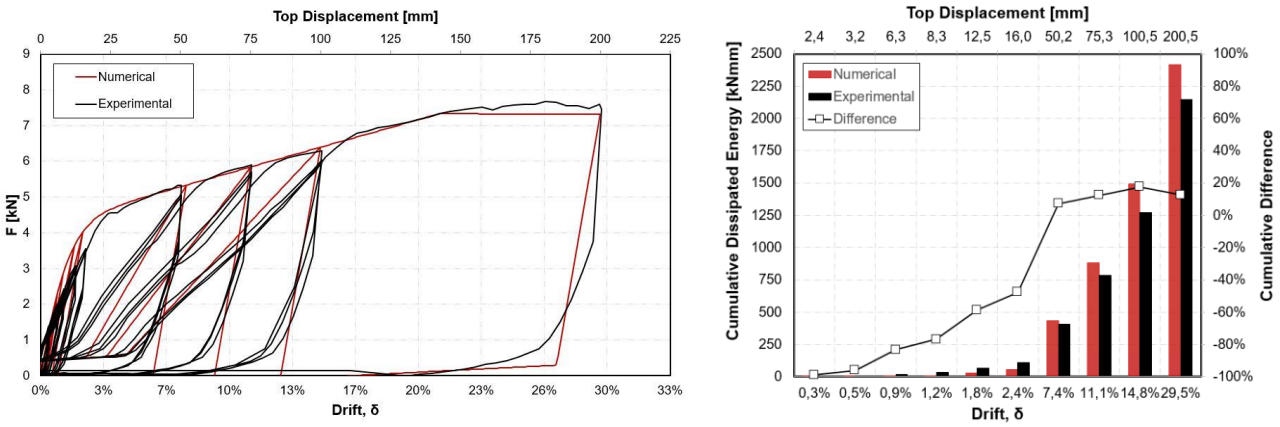

Figure 12 F-δ curve for tee-halved connection and cumulative dissipated energy (in-plane cyclic test).

4.2.2 An axial (2A) and a transversal (2T) spring simulating the relative displacements between the upper beam and posts

The two linear translational springs (2A, 2T in Figure 6) were modeled with *Elastic* uniaxial material with high stiffness to avoid any relative horizontal or vertical displacement between the upper beam and the posts based on the experimental observation.

4.3 Bracing's connections (3), and (4)

Since the wall stiffness is mainly controlled by diagonal elements, their connections (3) and (4) in Figure 6 were calibrated accurately to match the global envelope and, at the same time, the local damage mechanisms observed during the experimental test [18] such as vertical sliding along the external posts and diagonal detachment from the central lower connection described in Section 3.

The springs of upper and lower connections have two different alignments consistent with the related damage mechanisms: the first ones (3) are in accordance with the global axis while the lower ones are aligned along the center axis of the diagonals (4). The upper joint of the brace with external posts has three springs: two linear, horizontal and rotational (3H and 3R, respectively), and one nonlinear, vertical (3V). The horizontal spring (3H) was modeled with *Elastic* uniaxial material with high stiffness (1000 times the modulus of elasticity of timber elements) to have equal horizontal displacements between nodes, while the elastic stiffness of the rotational spring (3R) is very low (10^{-10} times less the modulus of elasticity of timber elements) resulting in negligible transfer of bending moments to model the behavior of truss elements.

The calibration of the elastic stiffness related to the nonlinear vertical (3V) spring was performed iteratively by comparing the experimental global response of the wall subjected to in-plane horizontal loading with the numerical one as well as controlling the sliding along the external post. This inverse fitting resulted in elastic

stiffness of 846 kN/m that was applied to the *Pinching4* uniaxial material whose hysteretic behavior is shown in Figure 13. The choice of this hysteretic material can be supported by the photos taken during the experimental test showing significant vertical sliding that increase the total dissipated energy through friction and yielding of the nails.

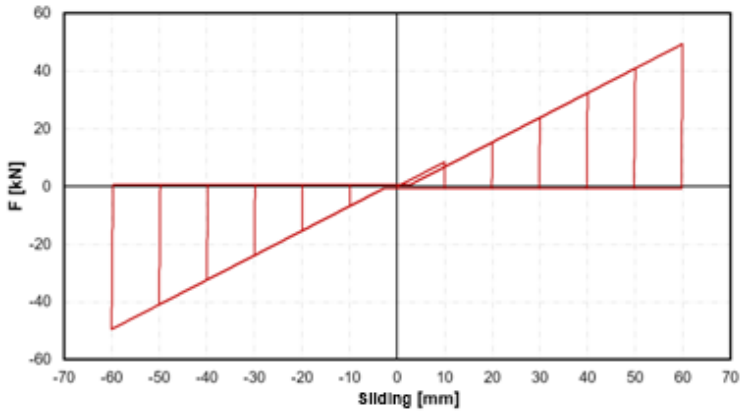

Figure 13 *Pinching4* material applied to the vertical nonlinear spring of diagonal elements.

Regarding the lower central connection between diagonals and post, (4) in Figure 6, it was modeled with three linear springs: the one oriented with the bracing center axis (4A) has an *Elastic-No Tension* uniaxial material with high stiffness to prevent the diagonals going through the post, the one perpendicular to the axis (4T) has high elastic stiffness applied to an *Elastic* uniaxial material, the rotational one (4R) has the same properties of the upper diagonal connection with low stiffness to prevent bending moment transmission. The choice of neglecting the tensile behavior of the lower diagonal connection is proven by the estimation of withdrawal capacity for slant nailing ($F_{ax,Rk}$) according to EN1995-1-1 [33] which results in a very low value of 0.0741 kN.

5 Numerical response of Romanian TFM wall (S1 Specimen)

The response of the proposed numerical model representing the Romanian TFM S1 Specimen was calibrated in two consecutive steps of analysis through an iterative procedure aimed at approaching the experimental outcomes in terms of envelope, damage mechanisms and deformed shape. This procedure required the updating of stiffness and strength parameters governing the nonlinear hysteretic behavior of the springs at the structural joints.

Nonlinear static analysis was performed before cyclic analysis to approach the global response in terms of initial and first yielding stiffness without considering stiffness and strength degradation related to cyclic loading. The global envelope of the experimental hysterical curve was determined by considering positive

displacements and base shear forces in Figure 5 as reference, to have an upper bound comparable with the resulting numerical pushover curves. Therefore, the yield point was estimated similarly to the procedure recommended by the European Committee for Standardization [34], assuming as secant line the one passing through the 38% peak load, namely the third cycle to neglect those highly influenced by the specimen setting and equipment testing, and as tangent line the one having one sixth of slope of that secant one. Among all the possible procedures to assess the yielding point of timber assemblies, this choice is justified by the fact that allows a certain range of values for the secant line (from 10% to 40% of peak load) since the envelope of the cyclic response does not present a softening branch so no reference peak load. Regarding the first yielding stiffness, its slope was determined by connecting the maximum base forces per cycles with the exception of those related to the horizontal displacement of 82 mm and to the last cycle. The imposed displacement of 82 mm was discarded since it is considered too close to the previous one (73.4 mm) according to the CUREE Caltech loading protocol [31], resulting in opposite trend with lower base force between consecutive peak displacements. The base force related to the last cycle was neglected as well, due to the accumulation of damages for large deformations resulting in severe stiffness and strength degradation.

The envelope was approached through the inverse fitting procedure modifying the initial stiffness of the nonlinear rotational springs of tee-halved and mortise and tenon connections, and also the stiffness of the vertical nonlinear spring in the upper connection between post and bracings. This process has been repeated until both initial and first yielding stiffness of the global response were comparable with the experimental curve, Figure 14. The resulting pushover curve defines the envelope of the experimental hysteretic curve except for the last cycle representing a second yielding stiffness that can be controlled by strength and stiffness degradation parameters of the connections during the second step of analysis.

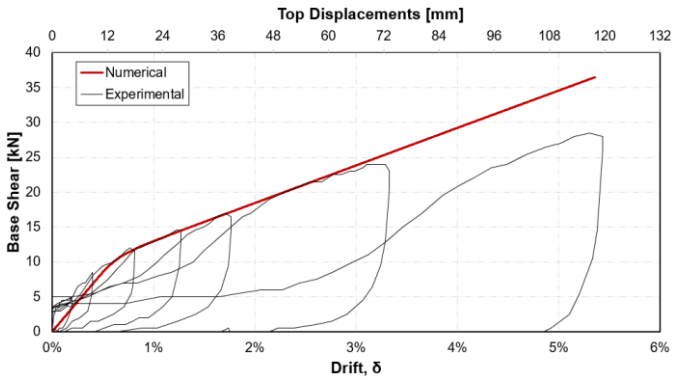

Figure 14 S1 Specimen pushover curve overlapped with experimental hysteretic curve.

The cyclic behavior of the tested wall was eventually calibrated by in-plane nonlinear cyclic analysis. In this case, the effect of strength and stiffness degradation influences significantly the global response, thus an additional updating of connections parameters was required to match the experimental curve. The analysis was performed by applying a vector of peak displacements based on those of the experimental test, neglecting the already mentioned displacement of 82 mm. This vector consists of maximum horizontal displacements with same values in both directions even though the positive and negative responses are not perfectly symmetric. This simplification may result in larger differences between experimental and numerical curves in terms of dissipated energy. The comparison is also influenced by the vertical shifting of experimental hysteretic curve that affect the dissipated energy calculation.

The experimental hysteretic curve was approached by modifying the rotational nonlinear springs of mortise and tenon and tee-halved connections in terms of yielding stiffness and intercept strength of the asymptotic line to the envelope curve. Figure 15a shows a good approximation in terms of maximum base shear per displacement-cycle peak and reloading stiffness between the numerical curve, highlighted in red, and the experimental one, in black. The main differences are related to the pinching effect and unloading branches which are comparable up to a certain point where the numerical stiffness changes its slope.

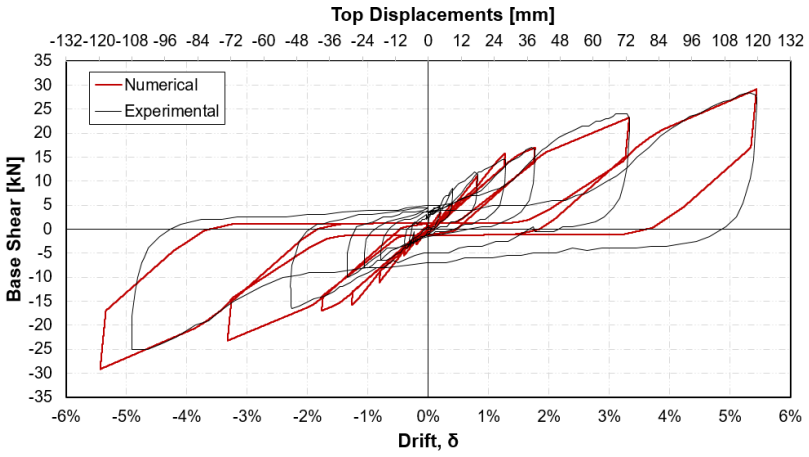

(a)

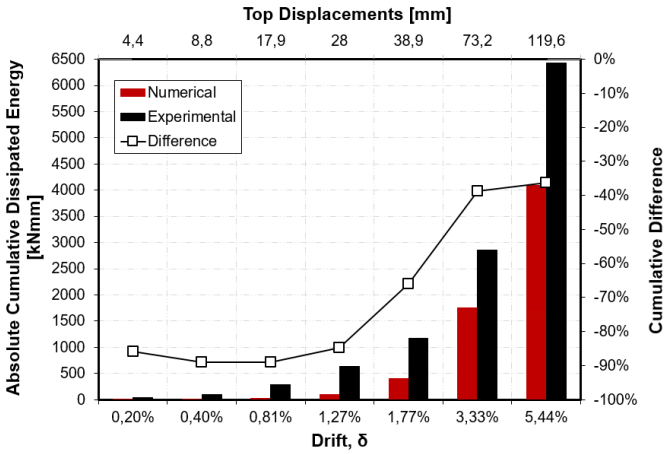

(b)

Figure 15 S1 Specimen cyclic analysis (a) and cumulative dissipated energy (b).

Figure 15b shows the cumulative dissipated energy and difference between the two curves. The cumulative difference ranges from -89% for negligible drifts to -36% for the maximum one (5.43%) with the numerical area always smaller than the experimental one due to the pinching effect and the vertical unloading of the experimental cycles. This depends on the physical behavior of the wall that returns instantly to its original position with no pressure by the horizontal jacks while the numerical model needs to be pushed to reach its starting condition.

The equivalent frame model overlapped with the deformed shape of Specimen S1 wall is pictured in Figure 16 with the expected behavior of diagonal bracings. The wall deformed as the tested one and showed a good approximation also in terms of damage pattern controlled by the sliding and detachment mechanisms of diagonal elements. In particular, the vertical sliding along the post is 63 mm, which is compatible with the experiment observations, Figure 17, while the observed diagonal detachment is lower than the numerical one (88-107 mm), Figure 18. This is due to the *Elastic-No Tension* material applied to the central lower connection and also on the stiffness of the upper vertical spring related to bracing-to-post connection, which was calibrated by assuming a vertical sliding around 65 mm based on experimental observation.

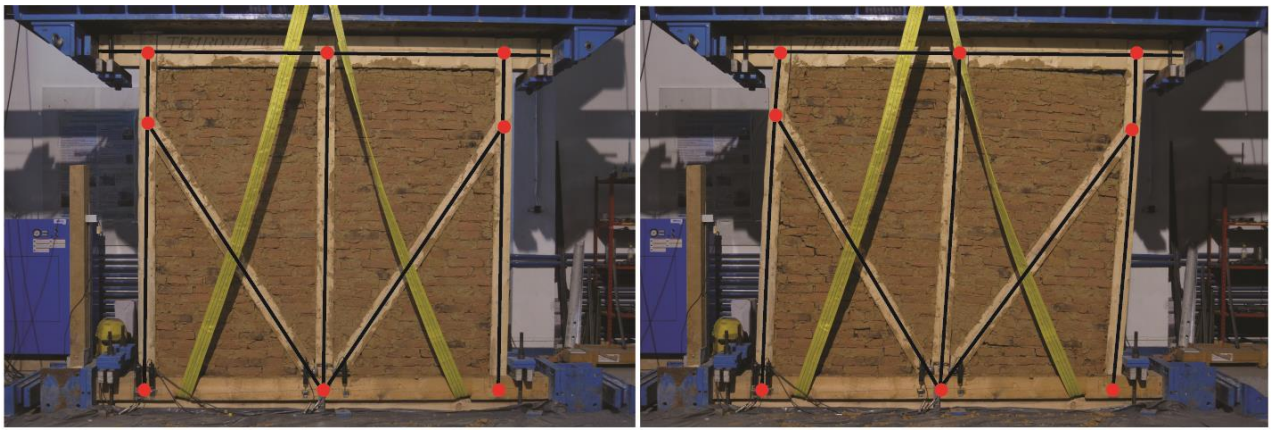

Figure 16 Initial step and final one during in-plane cyclic test.

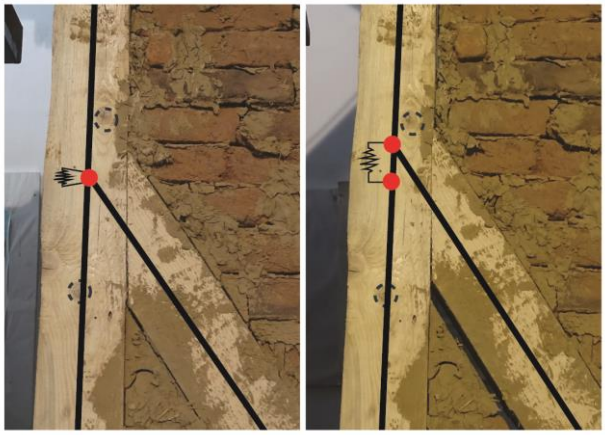

Figure 17 Vertical sliding along the post: initial and final position.

Figure 18 Detachment along the diagonal axis: initial and final position.

6 Comparison with Pombalino system

This section presents the application of the explained numerical approach to the Portuguese Pombalino TFM architecture focusing on the modeling issues and differences compared to the Romanian system. Moreover, the corresponding cyclic performances of both shear walls resulting from nonlinear cyclic analysis are compared to highlight the possibilities of the equivalent frame based model. The in-plane lateral response of the Portuguese TFM walls was investigated by means of numerical simulations by Lukic et al. [25] based on the experimental campaign by Poletti and Vasconcelos [11].

Bearing in mind that both systems can be defined as half-timber structures with masonry infill, but their building scale is not perfectly comparable (up to five stories for typical Portuguese constructions against one or two stories for the Romanian ones) [35], [36], the corresponding TFM panels consist of different arrangement of timber elements. Indeed the assembled frame for *gaiola pombalina* is stiffened by two diagonal members for each module and presents several cells along the height. However timber species are

similar for the two systems as well as timber joints although the typical mortise and tenon connections at the base of the Romanian panel are substituted by tee-halved ones for Pombalino walls, in which also half-lap cross-halved joint can be observed.

Despite these macroscopic differences, the equivalent frame based approach adopted by Lukic et al. [25] and in the present paper has demonstrated its reliability in simulating the seismic performance of the TFM shear walls tested by Poletti and Vasconcelos (Specimen UIW50 in [11]), and by Dutu et al. (Specimen S1 in [18]) of Figure 19. These walls present many differences such as: softwood species, Pinus Pinaster for Pombalino walls and fir for Romanian ones; global geometrical dimensions, 2.42x2.36 m and 3x2.4 m; arrangements of timber elements; type of masonry and related compressive strength, modern brick and mud fired brick units; external applied load, 150 kN and 26 kN; loading protocol, standard ISO 21581 and CUREE Caltech; and testing setup.

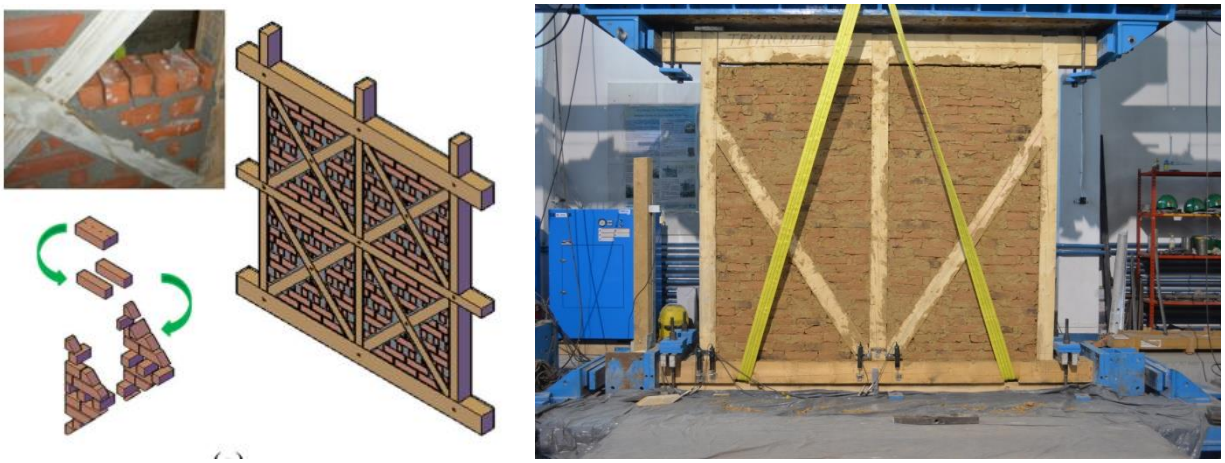

(a) **(b)**

Figure 19 Pombalino timber-framed wall (a) and Romanian one (b) with masonry infill [11].

In case of Pombalino wall, UIW50 Specimen in [11], the timber frame was again modeled with nonlinear beam elements with linear elastic constitutive laws while bracings were considered as trusses with the same elastic laws but neglecting shear deformations. Nonlinearities were still lumped at structural joints by means of zero-length nonlinear springs whose calibration was based on representative tests on half-lap joints, namely pull-out and in-plane cyclic tests [11], [15]. Brick masonry infill was not included as well, but its contribution was considered by updating the nonlinear springs applied at the base to limit the deformation capacity of joints.

The base connections present again the hysteretic material *Pinching4* for the vertical spring in parallel with an *Elastic-perfectly Plastic Gap* uniaxial material which shifts the response in compression through a gap (2

mm) simulating the presence of defects and possible damages during cyclic loading. Regarding the base rotational springs, the hysteretic material *SAWS* was adopted. These choices were made to model the post uplift observed during the experimental testing so the flexural rocking behavior of the wall. However the modeling of the bracing-to-post connections present some differences from those adopted in this paper because the global response was mostly controlled by flexural rocking at the base so nonlinearities were not applied in the central connection.

The hysteretic curves for Model 2 (Numerical) and Pombalino UIW50 Specimen in [11] (Experimental) is shown in Figure 20a. Even in the case of Pombalino wall, the numerical model can reproduce accurately the initial stiffness and strength capacity, but presents some limitations in the last cycles after 70 mm at which joint failure occurred and it was not simulated by the numerical model. The pinching effect due to the connection degradation for consecutive cycles is captured more precisely than the one in the Romanian wall, Figure 15a, at least before the joint failure. Moreover different maximum loads (100 kN for Pombalino and 29 kN for the Romanian wall) as well as drift ratios (4.0% and 5.3%) can be observed. This may be due to the higher load applied in the Portuguese wall and the higher performance of its masonry infill (modern brick units). The softening branch of the envelope in the Romanian wall cannot be observed because the maximum stroke of the actuator was reached in the testing sequence, thus the deformation capacity may exceed the measured one since no joint failure was registered. The unloading behavior of the two hysteretic curves is different as well. Indeed, the unloading branches of the Portuguese UIW50 Specimen present two steps with decreasing stiffness while, in the Romanian specimen, an immediate drop can be seen. This may be due to the different arrangement of diagonal elements and the additional division in cells. However this behavior was not accurately captured even by the numerical model by Lukic et al. [25]. Large asymmetry can be observed in both experimental curves which the numerical model cannot replicate. The Pombalino model overestimates the uplift by approximately 2.6 times at 66mm compared to the experimental one of 25mm (see Figure 20a) while the Romanian model simulates accurately the negligible uplift of external posts. When comparing the cumulative dissipated energy between the two walls, the one associated to the numerical model is always lower than the measured dissipated energy, but a similar trend of difference reduction can be observed both in Pombalino and Romanian walls, Figure 20b.

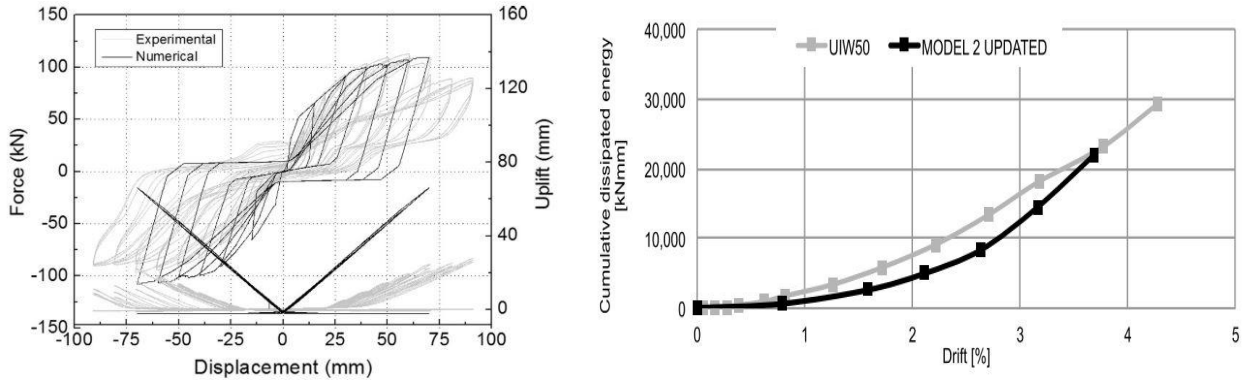

(a) **(b)**

Figure 20 Hysteresis curve of Pombalino Model 2 in [11] overlapped with the experimental one(a) and related cumulative dissipated energy (b) [25], [37].

Table 6 shows the estimated seismic parameters for the two specimens such as maximum drift, shear capacity, secant stiffness (at 40% of the maximum load) and ductility factor. Since they are all influenced by the applied vertical load, the comparison can be mostly qualitative also considering the geometrical and mechanical differences. The Pombalino wall has higher maximum shear capacity of the Romanian one that presents a larger drift ratio. The ductility factor is lower for UIW50 Specimen due to the higher level of pre-compression that changes the resisting mechanism from pure-shear to a mixed flexural-rocking one.

Table 6 Comparison of seismic parameters of Pombalino and Romanian wall.

Specimen	Drift [%]	Shear Capacity [kN]	Secant Stiffness [kN/mm]	Ductility Factor
UIW50 (Pombalino wall) in [11]	4.2	106	4.36	3.62
S1 panel (Romanain wall) in [17]	5.3	29	0.734	6.5

The response of the Portuguese wall (UIW50 Specimen) presents a predominant flexural-rocking behavior due to its aspect ratio and external load with significant uplift of the post (see Figure 21), while the Romanian one (S1 Specimen) shows a typical shear behavior with negligible uplift of vertical elements, but significant vertical sliding and detachment of diagonals. The detachment in tension was observed also in the bracings of Pombalino wall, but no sliding along the post was measured since these elements are aligned on the actual diagonal of the cells. Regarding the damage mechanisms, crushing of connections and detachment of masonry infill with out-of-plane movements were noticed in both walls. The Portuguese wall was damaged at the central joint (crushing of half-lap connection for post) and mostly in the lower part [38], Figure 22a, whereas the Romanian one experienced crushing in compression of the half-lap tee-halved connections at the top beam and additional damages due to the movement of its diagonals, Figure 22b. In conclusion, both mixed walls present good deformation capacity with controlled damages due to the

presence of masonry infill that confines timber members, prevents large shear deformations at the connections and increases the dissipated energy during dynamic loading.

(a) **(b)**

Figure 21 Local damages to Pombalino walls: uplift of external post (a) and related opening of connection (b) [38].

(a) **(b)**

Figure 22 Crushing at the central connection for Pombalino wall (a) and at the upper one for the Romanian one (b) [11], [18].

7 Conclusions

Timber-framed masonry architecture has already proven its effectiveness in seismic countries due to the empirical knowledge of local builders, but this background is no longer passed down nor its earthquake-resistant concepts are defined with science-based approaches. The potential lack of expertise and specific research should be prevented in particular for some countries such as Romania where this structural typology is widespread and still applied nowadays by technicians and non-specialized people. The research work continues the studies already conducted on Romanian timber-framed structures by performing numerical analysis on the cyclic behavior of TFM wall tested by Dutu *et al*. [18].

The Romanian TFM wall was modeled in the software OpenSEES as an equivalent frame structure with nonlinear properties lumped at the connections and no infill. Its global and local response was approached by

an iterative procedure of inverse fitting, starting from a preliminary calibration of the connections based on existing experimental tests on representative carpentry joints tested by Sakata *et al.* [28], and Dutu *et al.* [29] and passing through their further modification. This process can be time consuming without an automatic updating or if the response is controlled by many parameters, but it can provide reliable results and highlights the role of each connection and nonlinear-spring parameters. Moreover, nonlinear numerical analyses on simplified models do not require a large computational effort thus their application can be extended to the whole building.

The calibration of Romanian TFM wall was performed in two consecutive steps by comparing its experimental and numerical behavior when subjected to in-plane nonlinear static and cyclic analysis. The method of analysis influences the results since the nonlinear hysteretic uniaxial materials applied for the connections have parameters governing the stiffness and strength degradation per cycle. Moreover, varying the applied vertical load does not affect the global response due to the intrinsic properties of these adopted hysteretic materials, but these loads are representative of those in existing Romanian TFM structures. The resulting numerical hysteretic curve is not perfectly overlapped to the experimental one due to some limitations of the numerical model such as unloading and reloading stiffness, but the cyclic behavior is compatible also in terms of deformed shape and damage pattern. However, the proposed approach may be also adopted in future studies to the other typical Romanian walls, especially the one with masonry infill and corner-to-corner bracings, to investigate the differences in the modeling phase based on the response of structural connections.

Eventually, the Romanian system was compared with the Portuguese one with respect to the modeling issues in adopting the same equivalent frame based approach, as well as the resulting simulation of the seismic performance obtained with the experimental campaign by Poletti and Vasconcelos [11]. Despite presenting many differences, both structures share the basic principles of earthquake resistance which were applied based on available materials, techniques and knowledge. The seismic behavior of the tested Pombalino wall mostly depends on its flexural response showing severe damage at the central connection and large uplift at the external posts while a shear behavior can be observed for the Romanian wall with minor damages, namely diagonal detachment in tension and local compression perpendicular to grain direction in the upper joints. The capacity curve of Pombalino wall shows higher shear capacity and stiffness than the Romanian

one, but lower drift ratio and ductility factor due to the arrangement of its timber elements and masonry quality.

Acknowledgments

The authors wish to thank the University of Minho, where the research was carried out during the Master course in Structural Analysis of Monuments and Historical Constructions (SAHC program), and the Technical University of Civil Engineering of Bucharest – UTCB, where the experimental tests were performed.

References

[1] A. Bianco, *La casa baraccata: guida al progetto e al cantiere di restauro*. Rome, Italy: EditoriA, GB, 2010.

[2] N. Ruggieri, "An Italian anti-seismic system of the 18th century decay, failure modes and conservation principles," *Int. J. Conserv. Sci.*, vol. 7, no. Special Issue 2, pp. 827–838, 2016.

[3] D. I. Dima and A. Dutu, "Traditional buildings with timber frame and various infills in Romania," presented at the World Conference on Timber Engineering (WCTE), Vienna, Austria, 2016.

[4] P. Gülkan and R. Langenbach, "The earthquake resistance of traditional timber and masonry dwellings in Turkey," presented at the 13th World Conference on Earthquake Engineering (WCEE), Vancouver, B. C., Canada, 2004.

[5] T. Schacher, "Good engineering without appropriate communication doesn't lead to seismic risk reduction: some thoughts about appropriate knowledge transfer tools," presented at the 14th World Conference on Earthquake Engineering (WCEE), Beijing, China, 2008.

[6] R. Langenbach, *Don't tear it down: preserving the earthquake resistant vernacular architecture of Kashmir*. New Delhi, India: UNESCO, 2009.

[7] O. Sánchez, L. P. Kvist, and Z. Aguirre, "Bosques secos en Ecuador y sus plantas útiles," in *Botánica Económica de los Andes Centrales*, 2006, pp. 188–204.

[8] N. Quinn, "A seismic assessment procedure of historic structures," PhD Thesis, University College London (UCL), London, 2017.

[9] L. Holliday, T. Kang, and K. Mish, "Taquezal buildings in Nicaragua and their earthquake performance," *J. Perform. Constr. Facil.*, vol. 26, pp. 644–656, 2012, doi: 10.1061/(ASCE)CF.1943-5509.0000266.

[10] F. Vieux-Champagne, Y. Sieffert, S. Grange, A. Polastri, A. Ceccotti, and L. Daudeville, "Experimental analysis of seismic resistance of timber-framed structures with stones and earth infill," *Eng. Struct.*, vol. 69, pp. 102–115, 2014, doi: 10.1016/j.engstruct.2014.02.020.

[11] E. Poletti and G. Vasconcelos, "Seismic behaviour of traditional timber frame walls: experimental results on unreinforced walls," *Bull. Earthq. Eng.*, vol. 13, no. 3, pp. 885–916, 2015, doi: 10.1007/s10518-014-9650-9.

[12] S. Santos, "Ensaios de paredes pombalinas. (Tests of Pombalino walls). [in Portuguese]," Laboratório Nacional de Engenharia Civil (LNEC), Lisbon, Portugal, Technical Report no. 15/97-NCE, 1997.

[13] H. Meireles, "Seismic vulnerability of Pombalino buildings," PhD Thesis, Technical University of LIsbon, Lisbon, Portugal, 2012.

[14] A. M. Gonçalves, J. G. Ferreira, L. Guerreiro, and F. Branco, "Experimental characterization of Pombalino 'frontal' wall cyclic behaviour," presented at the 15th World Conference on Earthquake Engineering (WCEE), Lisbon, Portugal, 2012.

[15] E. Poletti, G. Vasconcelos, J. M. Branco, and A. M. Koukouviki, "Performance evaluation of traditional timber joints under cyclic loading and their influence on the seismic response of timber frame structures," *Constr. Build. Mater.*, vol. 127, pp. 321–334, 2016, doi: 10.1016/j.conbuildmat.2016.09.122.

[16] H. Meireles, R. Bento, S. Cattari, and S. Lagomarsino, "A hysteretic model for 'frontal' walls in Pombalino buildings," *Bull. Earthq. Eng.*, vol. 10, no. 5, pp. 1481–1502, 2012, doi: 10.1007/s10518-012-9360-0.

[17] A. Dutu, M. Niste, I. Spatarelu, D. I. Dima, and S. Kishiki, "Seismic evaluation of Romanian traditional buildings with timber frame and mud masonry infills by in-plane static cyclic tests," *Eng. Struct.*, vol. 167, pp. 655–670, 2018, doi: 10.1016/j.engstruct.2018.02.062.

[18] A. Dutu, M. Niste, and I. Spatarelu, "In-plane static cyclic tests on traditional Romanian houses' walls," presented at the 16th European Conference on Earthquake Engineering (ECEE), Thessaloniki, Greece, 2018.

[19] Y. Aktas, U. Akyuz, A. Turer, B. Erdil, and N. Şahin Güçhan, "Seismic resistance evaluation of traditional Ottoman timber-frame Hımış houses: frame loadings and material tests," *Earthq. Spectra*, vol. 30, pp. 1711–1732, 2014, doi: 10.1193/011412EQS011M.

[20] N. Ruggieri, G. Tampone, and R. Zinno, "In-plane versus out-of-plane 'behavior' of an Italian timber framed system - the Borbone constructive system: Historical analysis and experimental evaluation," *Int. J. Archit. Herit.*, vol. 9, no. 6, pp. 696–711, 2015, doi: 10.1080/15583058.2015.1041189.

[21] D. Torrealva and E. Vicente, "Experimental evaluation of seismic behavior of quincha walls from the historical centre of Lima – Peru.," presented at the 15th World Conference on Earthquake Engineering (WCEE), Lisbon, Portugal, 2012.

[22] L. A. S. Kouris and A. J. Kappos, "Detailed and simplified non-linear models for timber-framed masonry structures," *J. Cult. Herit.*, vol. 13, no. 1, pp. 47–58, 2012, doi: 10.1016/j.culher.2011.05.009.

[23] A. Ceccotti and C. Sandhaas, "A proposal for a standard procedure to establish the seismic behaviour factor q of timber buildings," presented at the World Conference on Timber Engineering (WCTE), 2010.

[24] B. Folz and A. Filiatrault, "Simplified seismic analysis of woodframe structures," presented at the 13th World Conference on Earthquake Engineering (WCEE), Vancouver, B. C., Canada, 2004.

[25] R. Lukic, E. Poletti, H. Rodrigues, and G. Vasconcelos, "Numerical modelling of the cyclic behavior of timber-framed structures," *Eng. Struct.*, vol. 165, pp. 210–221, 2018, doi: 10.1016/j.engstruct.2018.03.039.

[26] A. Dutu, H. Sakata, and Y. Yamazaki, "Experimental Study on Timber-Framed Masonry Structures," in *Historical earthquake-resistant timber frames in the Mediterranean area*, Springer, Cham, 2015, pp. 67–81.

[27] F. McKenna, G. L. Fenves, and M. H. Scott, *OpenSEES. Open System for Earthquake Engineering Simulation*. Berkeley: University of California, Pacific Earthquake Engineering Research Centre, 2000.

[28] H. Sakata, Y. Yamazaki, and Y. Ohashi, "A study on moment resisting behavior of mortise-tenon joint with dowel or split wedge," presented at the 15th World Conference on Earthquake Engineering (WCEE), Lisbon, Portugal, 2012.

[29] A. Dutu, M. Niste, I. Spatarelu, and D. I. Dima, "TFMRO project. Seismic evaluation of Romanian traditional residential buildings. [in Romanian]," Technical University of Civil Engineering of Bucharest, Scientific Report, 2017. [Online]. Available: http://tfmro.utcb.ro/.

[30] F. Pavel, R. Vacareanu, J. Douglas, M. Radulian, C. Cioflan, and A. Barbat, "An updated probabilistic seismic hazard assessment for Romania and comparison with the approach and outcomes of the SHARE project," *Pure Appl. Geophys.*, vol. 173, no. 6, pp. 1881–1905, 2016, doi: 10.1007/s00024-015-1223-6.

[31] H. Krawinkler, "Loading histories for cyclic tests in support of performance assessment of structural components," presented at the 3rd International Conference on Advances in Experimental Structural Engineering, Berkeley, CA, 2009.

[32] B. Folz and A. Filiatrault, *A computer program for seismic analysis of woodframe structures*, I. Richmond, California: Consortium of Universities for Research in Earthquake Engineering (CUREE), 2002.

[33] *EN 1995-1-1. Eurocode 5, Design of timber structures - Part 1-1, General - Common rules and rules for buildings*. 2004.

[34] *EN 12512:2001. Timber structures - test methods - cyclic testing of joints with mechanical fasteners. European Committee for Normalization, Brussels*. 2001.

[35] J. Mascarenhas, *Sistemas de Construção: V – O Edifício de Rendimento da Baixa Pombalina de Lisboa. (Constuction system V - Buildings in the Baixa Pombalina, Lisbon). [in Portuguese]*, 3ª. 2009.

[36] A. Duțu, D. I. Dima, and E. G. Bulimar, “Materials and techniques for traditional Romanian residential houses,” presented at the 3rd International Conference on Protection of Historical Constructions, Lisbon, Portugal, 2017.
[37] R. Lukic, “Numerical modeling of the cyclic behavior of Timber-framed structures,” Master Thesis, University of Minho, Guimarães, Portugal, 2016.
[38] E. Poletti, “Characterization of the seismic behavior of traditional timber frame walls,” PhD Thesis, University of Minho, Guimarães, Portugal, 2013.